

ARTICLE

Received 20 Jun 2012 | Accepted 31 Aug 2012 | Published 2 Oct 2012

DOI: 10.1038/ncomms2106

Linear magnetoresistance due to multiple-electron scattering by low-mobility islands in an inhomogeneous conductor

N.V. Kozlova^{1,2}, N. Mori³, O. Makarovskiy¹, L. Eaves¹, Q.D. Zhuang⁴, A. Krier⁴ & A. Patanè¹

Linear transverse magnetoresistance is commonly observed in many material systems including semimetals, narrow band-gap semiconductors, multi-layer graphene and topological insulators. It can originate in an inhomogeneous conductor from distortions in the current paths induced by macroscopic spatial fluctuations in the carrier mobility and it has been explained using a phenomenological semiclassical random resistor network model. However, the link between the linear magnetoresistance and the microscopic nature of the electron dynamics remains unknown. Here we demonstrate how the linear magnetoresistance arises from the stochastic behaviour of the electronic cycloidal trajectories around low-mobility islands in high-mobility inhomogeneous conductors and that this process is only weakly affected by the applied electric field strength. Also, we establish a quantitative link between the island morphology and the strength of linear magnetoresistance of relevance for future applications.

¹ School of Physics and Astronomy, The University of Nottingham, Nottingham NG7 2RD, UK. ² IFW Dresden, Institute for Metallic Materials, PO Box 270116, D-01171 Dresden, Germany. ³ Graduate School of Engineering, Osaka University, 2-1 Yamada-Oka, Suita City, Osaka 565-0871, Japan. ⁴ Department of Physics, Lancaster University, Lancaster LA1 4YB, UK. Correspondence and requests for materials should be addressed to A.P. (email: amalia.patane@nottingham.ac.uk).

Linear transverse magnetoresistance (MR) is a phenomenon commonly observed in many material systems, including semimetals¹, narrow band-gap semiconductors^{2,3}, multi-layer graphene⁴ and topological insulators⁵. Linear MR can arise from either quantum⁶ or classical effects^{7,8}. In particular, it can originate in an inhomogeneous conductor from distortions in the current paths induced by macroscopic spatial fluctuations in the carrier mobility; this type of non-saturating linear MR has been observed in several materials and explained in terms of a phenomenological semiclassical random resistor network model^{7,8}. However, the link between the linear MR and the microscopic nature of the electron dynamics remains still unexplored. Existing theories of classical linear MR apply to systems with ohmic conductivity, whereas the effects of hot electron dynamics on the linear MR are largely unknown. On the other hand, a significant enhancement of MR has been observed in the non-ohmic space-charge limited transport regime⁹ and under avalanche breakdown¹⁰, thus raising problems of fundamental interest and technological relevance, that is, what is the specific carrier dynamics giving rise to the linear MR, is it preserved in the presence of a large applied electric field and can it be controlled and exploited in sensitive Hall sensors or magnetoresistors¹¹?

Here, we examine the physical origin of the classical linear MR in a high-mobility inhomogeneous conductor. Our measurements and Monte Carlo simulations focus on the *n*-type compound semiconductor InAs and consider an extended range of applied electric (*E*) and magnetic (*B*) fields, and different sample geometries. By modelling our data with Monte Carlo simulations of the electron dynamics, we demonstrate that the linear MR arises from multiple scattering of the current-carrying electrons by low-mobility islands within the conducting layer. This process is only weakly affected by the details of the electronic band structure and electric field strength. Also, it persists at magnetic fields as high as ~50 T corresponding to a magnetic length as small as 4 nm, significantly smaller than the electron mean free path (~100 nm) and island size. The link between the linear MR and the stochastic behaviour of the electronic cycloidal trajectories around low-mobility islands is a finding of general interest as it is relevant to all high-mobility inhomogeneous conductors. The identification of a quantitative link between the island morphology and the strength of linear MR is also potentially useful for tailoring the linear MR in future applications.

Results

Material systems and devices. Our InAs and In(AsN) epilayers were grown by molecular beam epitaxy (MBE) on a semi-insulating (100)-oriented GaAs substrate. Owing to the mismatch between the substrate and epilayer lattices, inhomogeneities can arise due to the presence of dislocations and defects; also, the N-atoms act as scattering centres for the conduction electrons^{12,13}. Thus with increasing N-content from 0 to 1%, the electron Hall mobility decreases from $\mu_H = 3.3 \text{ m}^2 \text{ V}^{-1} \text{ s}^{-1}$ ($3.1 \text{ m}^2 \text{ V}^{-1} \text{ s}^{-1}$) to $0.6 \text{ m}^2 \text{ V}^{-1} \text{ s}^{-1}$ ($0.5 \text{ m}^2 \text{ V}^{-1} \text{ s}^{-1}$) at $T = 300 \text{ K}$ (4.2 K). Correspondingly, the electron density increases from $n_e = 4 \times 10^{16} \text{ cm}^{-3}$ in InAs to $n_e = 1.4 \times 10^{17} \text{ cm}^{-3}$ in In(AsN), with both values being very weakly affected by temperature.

The presence of inhomogeneous disorder combined with the high electron mobility makes these InAs and In(AsN) layers particularly well suited to the study of classical linear MR: even in the low-mobility layers the high values of $\mu B \gg 1$, which are necessary for observing a large MR, can be achieved with available conventional (superconducting) solenoids. To investigate the influence of sample geometry and electric field on the MR, two-terminal planar devices with InAs channels of length $L = 2, 5$ and $10 \mu\text{m}$ and of width $W = 1, 2$ and $5 \mu\text{m}$ were also studied.

High magnetic field studies. In our experiments, the magnetic field was applied parallel to the growth axis *z*, that is, $\mathbf{B} = [0, 0, B_z]$.

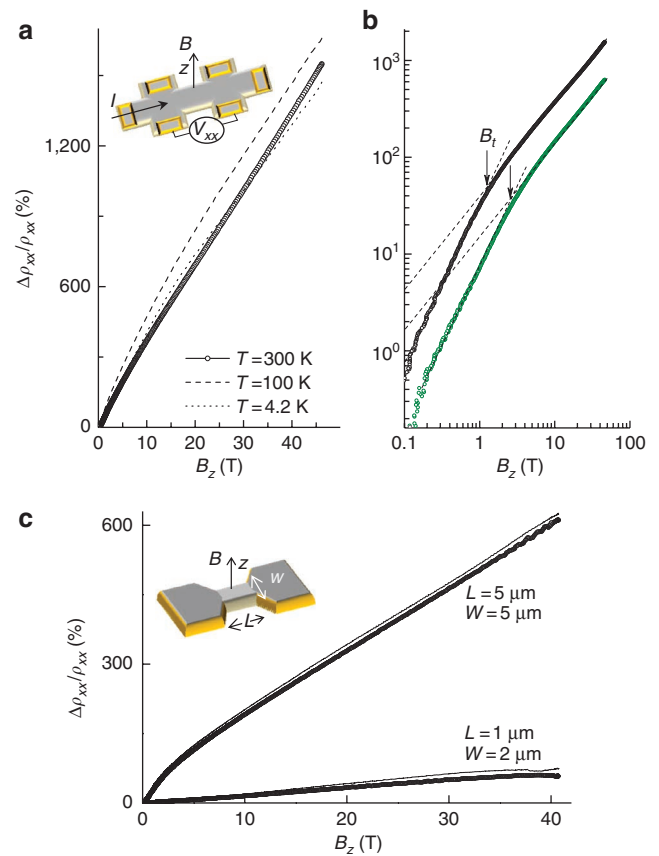


Figure 1 | Linear transverse MR in Hall bars and short-channel devices.

(a) Transverse MR, $\Delta\rho_{xx}/\rho_{xx}$, as a function of magnetic field, B_z , for an InAs Hall-bar at $T = 4.2, 100$ and 300 K . (b) $\Delta\rho_{xx}/\rho_{xx}$ as a function of B_z for InAs (black) and In(AsN) (green) Hall-bars ($T = 300 \text{ K}$). Dashed lines and arrows illustrate the transition of the dependence of $\Delta\rho_{xx}/\rho_{xx}$ on B_z from quadratic to linear at the characteristic magnetic field B_z^t . A linear fit to the MR data by the relation $\Delta\rho_{xx}/\rho_{xx} = \mu_0 B_z (s/2l)$ gives an average island coverage factor $f = 0.17$ and 0.32 in InAs and In(AsN), respectively. Here, s is the average size of the low-mobility regions, l is the inter-island separation and μ_0 is the zero field mobility. (c) $\Delta\rho_{xx}/\rho_{xx}$ versus B_z for short InAs channels of length, L , and width, W , at $T = 100 \text{ K}$ (line) and 300 K (symbols). The insets in panels (a) and (c) sketch a Hall-bar and a two-terminal planar device, respectively.

The transverse MR ratio defined as $\Delta\rho_{xx}/\rho_{xx} = [\rho_{xx}(B_z) - \rho_{xx}(0)]/\rho_{xx}(0)$ was studied with magnetic fields, B_z , up to 14 T, generated by a superconducting magnet, or in a pulsed solenoid at B_z up to 47 T with a total pulse length of 100 ms. Figure 1a shows the B_z -dependence of $\Delta\rho_{xx}/\rho_{xx}$ for an Hall-bar based on *n*-type InAs. A positive linear MR is observed at $B_z > 1 \text{ T}$ and is weakly affected by temperature in the range $T = 4.2\text{--}300 \text{ K}$. A weak oscillatory component of ρ_{xx} is observed at low temperature ($T < 20 \text{ K}$), which we attribute to the Shubnikov–de Haas effect in the two-dimensional electron gas that accumulates on the surface of InAs due to the bending of the conduction band by charged native surface defects¹². The resistance of the surface two-dimensional electron gas at $B_z = 0 \text{ T}$ is at least one order of magnitude higher than ρ_{xx} and, at all values of B_z and T , the amplitude of the magneto-oscillations is much smaller than the measured monotonically increasing MR.

Linear MR can occur when the electron distribution enters the so-called quantum limit, in which only the lowest Landau level is occupied, that is, when the cyclotron energy, $\hbar\omega_c$, exceeds the Fermi energy, ϵ_F , and when $\hbar\omega_c, \epsilon_F \gg k_B T$ (ref. 6). As shown in Fig. 1b,

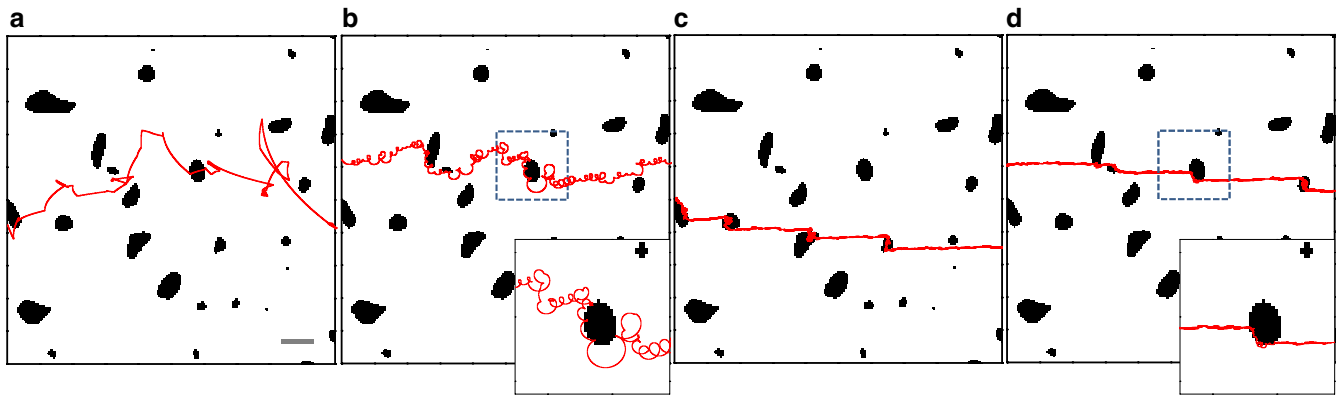


Figure 2 | Monte Carlo simulations of electron trajectories in magnetic field. Calculated electron trajectories (red lines) in InAs for an applied electric field $E_x = 0.5 \text{ kV cm}^{-1}$ and under various applied magnetic fields B_z : (a) $B_z = 0$, (b) 1, (c) 10 and (d) 20 T. The black areas correspond to regions of low mobility. As shown in the magnified trajectories in the insets of panels (b) and (d), in the vicinity of a low-mobility island, the electron undergoes multiple scattering events, which act to deflect the cycloidal motion. The bar in panel (a) corresponds to $1 \mu\text{m}$.

the transition of the MR to a linear B -dependence occurs at $B_z \sim 1 \text{ T}$ below the value satisfying the quantum limit condition $\hbar\omega_c = \varepsilon_F$, that is, $B_z = \hbar(3\pi^2 n_e)^{2/3}/2e$. This limit corresponds to fields $>3 \text{ T}$ for an electron density $n_e = 4 \times 10^{16} \text{ cm}^{-3}$, which we derive from the gradient of the Hall resistivity, ρ_{xy} , in the limit $B_z \rightarrow 0$. Also, we note that the condition for single occupancy of the lowest Landau level requires that $k_B T \ll \hbar\omega_c$. This condition is satisfied for temperatures $<50 \text{ K}$ at $B_z = 1 \text{ T}$ and for the electron cyclotron mass of InAs ($m_e = (0.025 \pm 0.01) m_0$, where m_0 is the electron mass in vacuum)¹⁴. However, the linear MR is observed well above $T = 50 \text{ K}$ (see Fig. 1), indicating that it does not have a quantum origin, but is a classical effect.

Classical linear MR has been explained using a phenomenological model in which the distorted current paths arising from disorder-induced inhomogeneities and macroscopic variations, $\Delta\mu$, in the electron mobility are simulated by a network of random resistors. Each resistor element has four terminals to take into account not only the local resistive voltage drop but also the Hall voltage associated with the local mobility, μ , of a particular region of the sample^{7,8}. The crossover of the MR from quadratic to linear B_z -dependence is predicted to occur at a characteristic magnetic field $B_z^t = \bar{\mu}^{-1}$ for $\Delta\mu/\bar{\mu} < 1$, or at $B_z^t = \Delta\mu^{-1}$ for $\Delta\mu/\bar{\mu} > 1$, where $\bar{\mu}$ corresponds to an average of the spatially varying mobility. A comparison of the B_z -dependence of $\Delta\rho_{xx}/\rho_{xx}$ in our InAs and In(AsN) Hall-bars at $T = 300 \text{ K}$ (see Fig. 1b) shows that both the value of $1/B_z^t$ and the slope of the MR follow the systematic decrease of μ from $3.3 \text{ m}^2 \text{ V}^{-1} \text{ s}^{-1}$ in InAs to $0.6 \text{ m}^2 \text{ V}^{-1} \text{ s}^{-1}$ in In(AsN). The characteristic magnetic field B_z^t provides an estimate of the average mobilities $\bar{\mu} = 1/B_z^t \sim 1 \text{ m}^2 \text{ V}^{-1} \text{ s}^{-1}$ and $0.5 \text{ m}^2 \text{ V}^{-1} \text{ s}^{-1}$ in the InAs and In(AsN) samples, respectively, which are comparable with those measured by the Hall effect. Also, the MR tends to follow the temperature dependence of μ : in the InAs sample, an increase of $T > 4.2 \text{ K}$ and up to $T \sim 100 \text{ K}$ leads to an increase of μ_H from 3.1 to $3.8 \text{ m}^2 \text{ V}^{-1} \text{ s}^{-1}$ followed by a decrease at $T > 150 \text{ K}$. This variation is caused by the interplay between impurity and phonon scattering and is accompanied by a similar T -dependence of the MR (see Fig. 1a). Linear MR is also observed in the two-terminal small channel devices, see Fig. 1c.

Monte Carlo simulations. As our InAs and In(AsN) epilayers are grown on highly lattice-mismatched GaAs, threading dislocations tend to form at the epilayer/substrate interface. The macroscopic ($>0.1 \mu\text{m}$) inhomogeneities observed by transmission electron microscopy of our samples¹⁵ are likely to induce variations in the electronic properties. We model the effect of such inhomogeneities

on the electron dynamics by Monte Carlo simulations¹⁶. As the magnetic field is applied along the z -direction, the magnetic field affects the components of the electron motion in the x - y plane. In our simulation of the two-dimensional electron trajectories, inhomogeneity is introduced by placing low-mobility islands randomly within the x - y plane (Fig. 2). The random spatial profile of the islands, $\Delta(x, y)$, is generated from the power spectrum of the autocorrelation function $\langle \Delta(\mathbf{r})\Delta(\mathbf{r}') \rangle = \Delta^2 \exp[-|\mathbf{r} - \mathbf{r}'|^2/\Lambda^2]$, where Λ is the correlation length, $\mathbf{r} = (x, y)$ and $\mathbf{r}' = (x', y')$. The low-mobility regions R_{low} are then defined according to the relation $R_{\text{low}} = \{ \mathbf{r} | \Delta(\mathbf{r}) < \Delta_{\text{th}} \}$. This condition determines the fractional area, f , of the sample with low mobility in which electrons undergo scattering at a rate higher than in the remaining high-mobility part of the sample. In a three-dimensional model, the value of f would result from an average of the f -values from various x - y planes of the three-dimensional conducting channel. In the low-mobility regions, we use a scattering rate $r_{\text{island}} = r_i + r_e$, where $r_i = 1.5 \times 10^{12} \text{ s}^{-1}$ and $r_e = 2.5 \times 10^{14} \text{ s}^{-1}$ are the elastic and inelastic phonon scattering rates, respectively; elsewhere, the electron drift is mainly limited by inelastic scattering with $r \sim r_i$. The non-parabolicity of the electron energy dispersion of InAs is modelled as $\varepsilon(\mathbf{k})[1 + \alpha\varepsilon(\mathbf{k})] = \hbar^2 k^2/2m_e$, where $m_e = 0.026 m_0$ and $\alpha = 2.2 \text{ eV}^{-1}$. This form of the energy dispersion occurs in numerous semiconductors, including the narrow gap InSb for which observations of linear MR have been also reported^{2,3}. The electron velocity, given by $\mathbf{v}(\mathbf{k}) = \hbar^{-1} \nabla_{\mathbf{k}} \varepsilon$, and the wave vector, \mathbf{k} , change with time under the action of the Lorentz force, $\mathbf{F} = -e[\mathbf{E} + \mathbf{v} \times \mathbf{B}]$, where $\mathbf{E} = [E_x, E_y, 0]$ and $\mathbf{B} = [0, 0, B_z]$ ¹⁷. The Hall field component, E_y , is set so that the y -component of the average electron velocity is zero, that is, $\mathbf{v} = [v_x, 0, 0]$, consistent with the current flow for our Hall bars. The main findings of our simulations are not changed if we consider a different geometry in which the Hall field is effectively 'shorted out', that is, $E_y = 0$. Thus, our analysis applies not only to Hall-bars but also to short channels and Corbino geometries, in which the Hall electric field is fully 'short-circuited' by the contact electrodes.

Figure 2a-d illustrates the calculated electron trajectories at $E_x = 0.5 \text{ kV cm}^{-1}$ and $B_z = 0, 1, 10$ and 20 T . Here, we have assumed a correlation length $\Lambda = 0.5 \mu\text{m}$, $f = 5\%$ and low-mobility regions of average size $s = 0.4 \mu\text{m}$ and inter-island separation $l = 8 \mu\text{m}$. It can be seen that in the vicinity of the low-mobility islands, the electron undergoes multiple scattering events, which act to deflect the cycloidal motion (see inset of Fig. 2b). This island-induced scattering is observed at low (Fig. 2b) and high (Fig. 2d) applied magnetic fields. It is absent in a homogenous system and is responsible for the linear magnetic field dependence of the inverse mobility component, μ_{xx}^{-1} , whose strength increases with f , as shown in Fig. 3a.

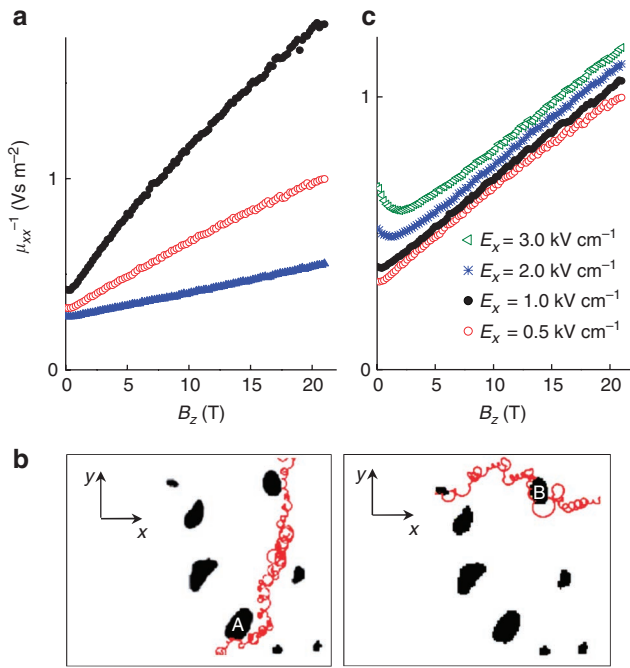


Figure 3 | Monte Carlo simulations of the electron mobility and its magnetic field dependence. (a) Dependence of the inverse of the mobility, μ_{xx}^{-1} on magnetic field, B_z , in InAs at various values of the island coverage factor $f = 0.1$ (black), $f = 0.05$ (red) and $f = 0.02$ (blue). (b) Calculated electron trajectories (red lines) in InAs at $B_z = 1$ T, $E_x = 0.5$ kV cm⁻¹ and different electric field components E_y (left: $E_y = 0$ and $v_y = 5 \times 10^4$ m s⁻¹; right: $E_y = 1.5$ kV cm⁻¹ and $v_y = 0$). The black areas show regions of low mobility. A and B indicate two typical islands. (c) Dependence of μ_{xx}^{-1} on E_x for $f = 0.05$.

Discussion

We interpret the results of the Monte Carlo simulations by considering a simplified Drude model of the average electron velocity v_x and average hopping distance travelled by the conduction electrons along the x -direction. In a uniform system, that is, with no islands, and for $E_y = 0$ and $v_y \neq 0$, the average velocity along x is $v_x = \Delta X / \tau$, where $\Delta X \equiv m_e |E_x| / (eB_z^2)$ is the typical hopping distance and τ is the scattering time. In the presence of inhomogeneity, an electron travels an additional distance $\Delta X' \sim s/2$ around a low-mobility island. As the electron hits an island every time interval $\tau_{\text{island}} \sim l/v_H$, where $v_H = E_x/B_z$ is the electron Hall velocity along y and l is the distance between the islands, the average electron velocity v_x and mobility component μ_{xx} increase as $v_x = \Delta X / \tau + \Delta X' / \tau_{\text{island}}$ and $\mu_{xx} = m_e / (\tau e^2 B_z^2) + s / (2l B_z)$, respectively. Thus, if we compare this result with the case of an homogenous system for which $\mu_{xx} = m_e / (\tau e^2 B_z^2)$ and $v_x = m_e |E_x| / (\tau e B_z^2)$, we conclude that at high B_z island scattering tends to facilitate electron drift along the x -direction, perpendicular to the cycloidal motion along y (see electron scattering around island A in Fig. 3b).

For the geometry in which $E_y = 0$ and $v_y \neq 0$, the resistivity component ρ_{xx} is given by $\rho_{xx} = E_x / J_x = 1 / ne \mu_{xx}$. Using the dependence of μ_{xx} on B_z at large fields, that is, $\mu_{xx} \sim \Delta X' / \tau_{\text{island}} = s / (2l B_z)$, we derive a linear MR, that is, $\Delta \rho_{xx} / \rho_{xx} \sim B_z \mu^*$, where $\mu^* = \mu_0 (s/2l)$ is an effective mobility and μ_0 is the zero field mobility. A similar conclusion can be drawn for the Hall geometry, that is, for $E_y \neq 0$ and $v_y = 0$. In this case the resistivity component ρ_{xx} is given by $\rho_{xx} = \mu_{xx} / [ne(\mu_{xx}^2 + \mu_{xy}^2)]$, where $\mu_{xy} = B_z^{-1}$. Using this expression in the limits of high B_z , we obtain also in this case that $\Delta \rho_{xx} / \rho_{xx} \sim B_z \mu^*$. Note, however, that in this geometry, the island scattering acts to decrease the average electron velocity, v_x , by deflecting the

electron motion along y (see electron scattering around island-B in Fig. 3b).

In summary, the magnetic field dependence of the mobility component μ_{xx} due to island scattering generates a characteristic linear dependence of the MR on magnetic field, which is the same in both geometries, that is, $E_y \neq 0$ and $E_y = 0$. This analysis identifies the physical origin of the random variation of the resistive and Hall effect components of each four-terminal resistive element of the network model^{7,8}: the randomness arises from the stochastic behaviour of the electronic cycloidal trajectories around the low-mobility islands.

From a linear fit to the measured MR data for the large InAs Hall-bar of Fig. 1b by the relation $\Delta \rho_{xx} / \rho_{xx} = B_z \mu^*$, we obtain $\mu^* = 0.33$ m² V⁻¹ s⁻¹. For $\mu_0 = \mu_H = 3.3$ m² V⁻¹ s⁻¹, this corresponds to $s/(2l) = \mu^* / \mu_0 = 0.1$ and an average island coverage factor $f = s/(s+l) \sim 0.17$. Similarly, for the In(AsN) Hall-bar of Fig. 1b we find that $s/(2l) = \mu^* / \mu_0 = 0.23$ and $f = s/(s+l) \sim 0.32$. Thus, in both cases the average island separation, l , is significantly larger than the average island size, s . Although we cannot deduce the exact value of l or s , we can infer a reasonable estimate from our MR experiments in small channel devices, see Fig. 1c. Here, it can be seen that devices with small values of the channel length L (2–10 μ m) and/or width W (1–5 μ m) exhibit much smaller values of $\Delta \rho_{xx} / \rho_{xx}$ and in the smallest devices the MR tends to saturate at high B_z . The linear MR decreases systematically as the channel width W and length L decrease to values of the order of 1 μ m. Thus, we infer that the dimensions of these small devices are comparable to the average island separation.

The Monte Carlo simulations indicate that different values of the band non-parabolicity parameter α produce similar linear MR behaviour. Thus, the specific details of the electronic band structure do not have a critical role in the observation of linear MR. Perhaps surprisingly, although μ_{xx}^{-1} tends to increase with increasing E_x , its linear dependence on B_z is found to be weakly affected by electric field (Fig. 3c) and only at low-magnetic fields (< 1 T) and high E_x does the value of μ_{xx}^{-1} tend to decrease with decreasing B_z , thus leading to a weak negative MR. This is caused by the interplay between electron cyclotron motion and island-induced scattering, which tends to be increased by E_x , that is, electrons hit a low-mobility islands more frequently at higher speeds. However, overall this effect tends to be weak and, at large B_z , the deflection of the cycloidal motion by the low-mobility islands and corresponding linear MR are preserved.

The weak dependence of the linear MR on applied electric field is confirmed by our MR experiments in the short channel InAs samples. Figure 4a shows the dependence of the current density J on E_x at low temperature ($T = 4.2$ K) and at various B_z (up to 14 T) for an InAs channel of length $L = 10$ μ m and width $W = 2$ μ m. Similar dependences of J on E_x and B_z were found in devices with different values of L and W . At $B_z = 0$ T, the $J(E_x)$ curve is approximately linear at low bias. The ohmic behaviour is then followed by a slight sublinear bias dependence and, at larger electric fields, by a sharp rise of the current that is characteristic of systems switching from a state of low to high conductivity due to impact ionization and avalanche breakdown^{15,18}. At all values of E_x , the magnetic field acts to suppress the current and to shift the threshold electric field for impact ionization to significantly higher values. From Fig. 4b, it can be seen that the MR remains linear over an extended range of E_x up to ~ 3 kV cm⁻¹, just below the threshold electric field for impact ionization. In contrast, in the regime of avalanche breakdown the MR is strongly enhanced and tends to depart from a simple linear dependence due to the effect of the magnetic field in suppressing the avalanche multiplication of carriers¹⁰.

To conclude, our data and analysis indicate that the presence of low-mobility islands in a high-mobility conductor and their effect on the electron trajectories underpin the observation of classical

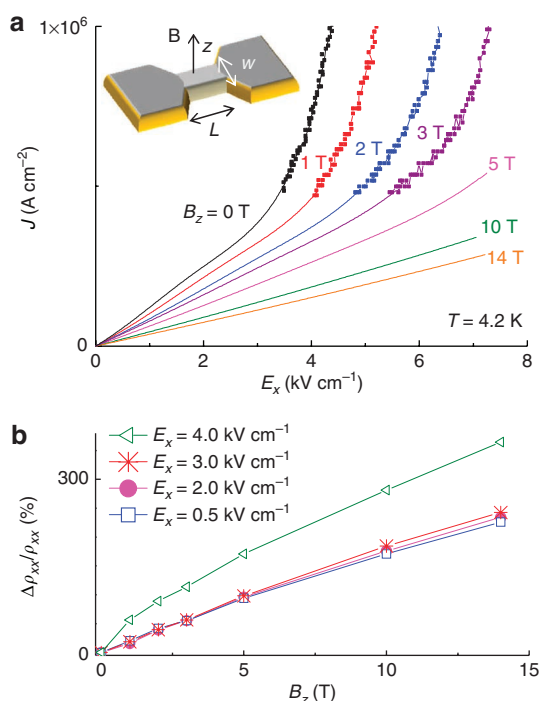


Figure 4 | Linear transverse MR at high electric fields. (a) Dependence of the current density J on electric field E_x at various magnetic fields B_z for an InAs channel of length $L = 10\ \mu\text{m}$ and width $W = 2\ \mu\text{m}$ ($T = 4.2\ \text{K}$). Measurements of the $J(E_x)$ characteristics were performed in both the direct current (lines) and pulsed mode (symbols). The inset sketches a two-terminal planar device. (b) Transverse MR, $\Delta\rho_{xx}/\rho_{xx}$ as a function of B_z at various values of E_x . The resistivity ρ_{xx} is calculated as $\rho_{xx} = E_x/J$.

linear MR. We have established a clear link between the stochastic dynamics of the electron trajectory around low-mobility islands caused by multiple scattering at the islands and the classical linear MR in devices with different geometry and size. Although our observations have focused on the high-mobility inhomogeneous n -type InAs and In(AsN) epilayers grown on GaAs, our main findings and conclusions are relevant to a wide variety of structures, device geometries and material systems. Our results are therefore of general interest and will help guiding future research into the manipulation of the linear MR by tuning of the electron trajectories in tailor-made inhomogeneous materials and device structures.

Methods

Growth and fabrication. Our InAs epilayer (thickness $t = 1.5\ \mu\text{m}$) was grown by MBE on a semi-insulating (100)-oriented GaAs substrate. An In(AsN) epilayer ($t = 1.3\ \mu\text{m}$) containing a small concentration ($N = 1\%$) of substitutional N-atoms was also grown by MBE using a radio frequency (RF) plasma N-source. The surface reconstruction was monitored by *in situ* reflection high-energy electron diffraction, while the substrate temperature was measured using an infrared pyrometer calibrated with the surface reconstruction transitions at a fixed As-flux. A Veeco UNI-Bulb RF plasma source was used as nitrogen source. It was set at a RF power of 160 W with a nitrogen flux of 5×10^{-6} mbar for all epilayers. The N-content in the In(AsN) epilayers and the crystal quality of the layers were optimized by setting the growth temperature, T_G , and the growth rate, r_G , to given values in the ranges $T_G = 400\text{--}460\ \text{°C}$ and $r_G = 0.3\text{--}1\ \mu\text{m h}^{-1}$, and by keeping a minimum As-flux. The InAs epilayer was grown at $T_G = 460\ \text{°C}$. High-resolution X-ray diffraction measurements using a Bede QC200 diffractometer confirmed a relaxation of the crystal lattice by 98% in the InAs and In(AsN) epilayers.

The wafers were spun with photoresist and patterned by photolithography into Hall-bars of length $L = 1,250\ \mu\text{m}$ and width $W = 250\ \mu\text{m}$. Two-terminal planar devices with InAs channels of length $L = 2, 5$ and $10\ \mu\text{m}$ and of width $W = 1, 2$ and $5\ \mu\text{m}$ were also fabricated by electron beam lithography. Each channel was formed by dry-etching the epilayer down to the GaAs substrate. Metal contacts consisting of 10 nm of Ti followed by 200 nm of Au were deposited onto the samples to provide Ti–Au ohmic contacts.

Transport studies. Measurements of the current–voltage characteristics were performed in both direct current and pulsed mode. For the pulsed mode of acquisition of the current, a voltage pulse generator was used to generate saw-tooth single voltage pulses of duration of $10\ \mu\text{s}$, and a digital oscilloscope was used for the synchronized and fast temporal recording of the applied bias and current, thus reducing excessive sample heating at high-operating currents. The current–voltage curves in pulsed magnetic field were taken within 1 ms at the top of the magnetic field pulse, during which the magnetic field remains constant to within $\pm 0.5\%$.

References

- Xu, R. *et al.* Large magnetoresistance in non-magnetic silver chalcogenides. *Nature* **390**, 57–60 (1997).
- Hu, J. & Rosenbaum, T. F. Classical and quantum routes to linear magnetoresistance. *Nat. Mater.* **7**, 697–700 (2008).
- Branford, W. R. *et al.* Geometric manipulation of the high-field linear magnetoresistance in InSb epilayers on GaAs (001). *Appl. Phys. Lett.* **86**, 202116 (2005).
- Friedman, A. L. *et al.* Quantum linear magnetoresistance in multilayer epitaxial graphene. *Nano Lett.* **10**, 3962–3965 (2010).
- Zhang, W. *et al.* Topological aspect and quantum magnetoresistance of β -Ag₂Te. *Phys. Rev. Lett.* **106**, 156808 (2011).
- Abrikosov, A. A. Quantum linear magnetoresistance; solution of an old mystery. *J. Phys. A Math. Gen.* **36**, 9119–9131 (2003).
- Parish, M. M. & Littlewood, P. B. Non-saturating magnetoresistance in heavily disordered semiconductors. *Nature* **426**, 162–165 (2003).
- Parish, M. M. & Littlewood, P. B. Classical magnetotransport of inhomogeneous conductors. *Phys. Rev. B* **72**, 094417 (2005).
- Demo, M. P., Yamamoto, S., Kasai, S., Ono, T. & Kobayashi, K. Large positive magnetoresistive effect in silicon induced by the space-charge effect. *Nature* **457**, 1112–1115 (2009).
- Sun, Z. G., Mizuguchi, M., Manago, T. & Akinaga, H. Magnetic-field-controllable avalanche breakdown and giant magnetoresistive effects in gold/semi-insulating-GaAs Schottky diode. *Appl. Phys. Lett.* **85**, 5643–5645 (2004).
- Heremans, J. Solid state magnetic field sensors and applications. *J. Appl. Phys.* **26**, 1149–1168 (1993).
- Patanè, A. *et al.* Effect of low nitrogen concentrations on the electronic properties of InAs_{1-x}N_x. *Phys. Rev. B* **80**, 115207 (2009).
- Fahy, S., Lindsay, A., Ouerdane, H. & O'Reilly, E. P. Alloy scattering of n -type carriers in GaN_xAs_{1-x}. *Phys. Rev. B* **74**, 035203 (2006).
- Drachenko, O. *et al.* Cyclotron resonance mass and Fermi energy pinning in the In(AsN) alloy. *Appl. Phys. Lett.* **98**, 162109–162111 (2011).
- Makarovsky, O. *et al.* Hot electron transport and impact ionization in the narrow energy gap InAs_{1-x}N_x alloy. *Appl. Phys. Lett.* **96**, 052115–052118 (2010).
- Jacoboni, C. & Reggiani, L. The Monte Carlo method for the solution of charge transport in semiconductors with applications to covalent materials. *Rev. Mod. Phys.* **55**, 645–705 (1983).
- Hamaguchi, C. *Basic Semiconductor Physics* 46 (Springer-Verlag, London, 2006).
- Fischetti, M. V. Monte Carlo simulation of transport in technologically significant semiconductors of the diamond and zinc-blende structures. 1. Homogeneous transport. *IEEE Trans. Electron Dev.* **38**, 634–649 (1991).

Acknowledgements

This work was supported by the Royal Society (UK), DFG KO 3743/1-1, AOBJ: 550341. We acknowledge Dr R. Airey (EPSRC, III-V National Facility, Sheffield) for processing our samples.

Author contributions

A.P., N.V.K. and O.M. designed and performed the experiments; N.M. performed the Monte Carlo simulations; L.E. took part in the discussions of the Monte Carlo studies; A.K. and Q.D.Z. grew the samples; A.P. wrote the paper; and all authors took part in the discussion/analysis of the data.

Additional information

Competing financial interests: The authors declare no competing financial interests.

Reprints and permission information is available online at <http://npg.nature.com/reprintsandpermissions/>

How to cite this article: Kozlova, N.V. *et al.* Linear magnetoresistance due to multiple-electron scattering by low-mobility islands in an inhomogeneous conductor. *Nat. Commun.* **3**:1097 doi: 10.1038/ncomms2106 (2012).

License: This work is licensed under a Creative Commons Attribution-NonCommercial-Share Alike 3.0 Unported License. To view a copy of this license, visit <http://creativecommons.org/licenses/by-nc-sa/3.0/>